Supplement of Biogeosciences, 23, 5477–5495, 2026
https://doi.org/10.5194/bg-23-5477-2026-supplement

Biogeosciences
Open Access

Supplement of

Planktonic foraminifera iodine / calcium ratio: is it a proxy for dissolved oxygen in the ocean?

Vincent Guarinos et al.

Correspondence to: Vincent Guarinos (guarinos@cerege.fr)

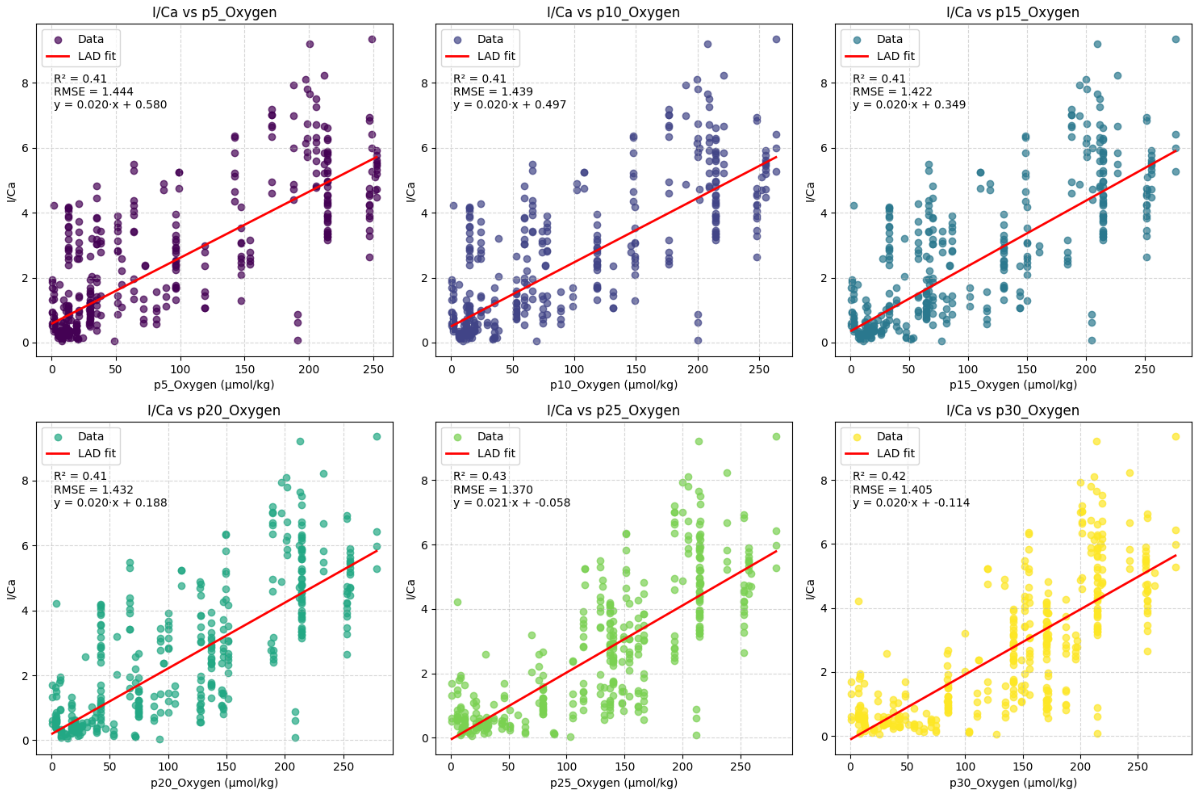

<u>Figure S1:</u> Foraminiferal I/Ca as a function of 5th, 10th, 15th, 20th, 25th, and 30th percentiles of [O_2] (µmol/kg). R^2, RMSE and equations are shown for each subplot. The figure represents core top data more recent than 2 ka BP.

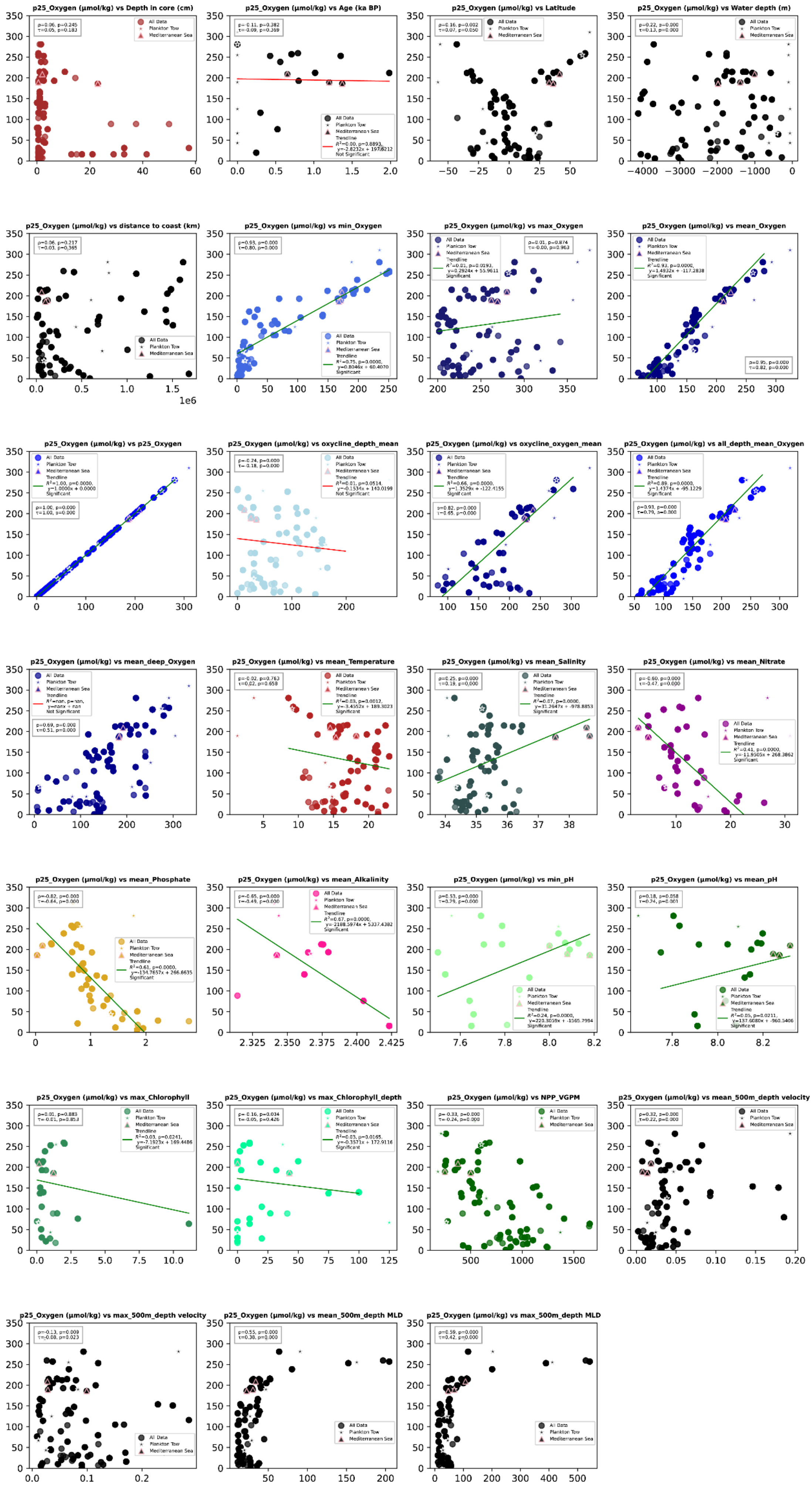
p25_Oxygen (µmol/kg) vs Depth in core (cm)
p25_Oxygen (µmol/kg) vs Age (ka BP)
p25_Oxygen (µmol/kg) vs Latitude
p25_Oxygen (µmol/kg) vs Water depth (m)
p25_Oxygen (µmol/kg) vs distance to coast (km)
p25_Oxygen (µmol/kg) vs min_Oxygen
p25_Oxygen (µmol/kg) vs max_Oxygen
p25_Oxygen (µmol/kg) vs mean_Oxygen
p25_Oxygen (µmol/kg) vs p25_Oxygen
p25_Oxygen (µmol/kg) vs oxycline_depth_mean
p25_Oxygen (µmol/kg) vs oxycline_oxygen_mean
p25_Oxygen (µmol/kg) vs all_depth_mean_Oxygen
p25_Oxygen (µmol/kg) vs mean_deep_Oxygen
p25_Oxygen (µmol/kg) vs mean_Temperature
p25_Oxygen (µmol/kg) vs mean_Salinity
p25_Oxygen (µmol/kg) vs mean_Nitrate
p25_Oxygen (µmol/kg) vs mean_Phosphate
p25_Oxygen (µmol/kg) vs mean_Alkalinity
p25_Oxygen (µmol/kg) vs min_pH
p25_Oxygen (µmol/kg) vs mean_pH
p25_Oxygen (µmol/kg) vs max_Chlorophyll
p25_Oxygen (µmol/kg) vs max_Chlorophyll_depth
p25_Oxygen (µmol/kg) vs NPP_VGPM
p25_Oxygen (µmol/kg) vs mean_500m_depth velocity
p25_Oxygen (µmol/kg) vs max_500m_depth velocity
p25_Oxygen (µmol/kg) vs mean_500m_depth MLD
p25_Oxygen (µmol/kg) vs max_500m_depth MLD

Figure S2: p25 [O_2] (µmol/kg) as a function of environmental parameters. Mediterranean and plankton tow sites data have been separated from previously published dataset and are highlighted in the figure. Spearman's and Kendall's correlation coefficients with p-values are associated with each plot.

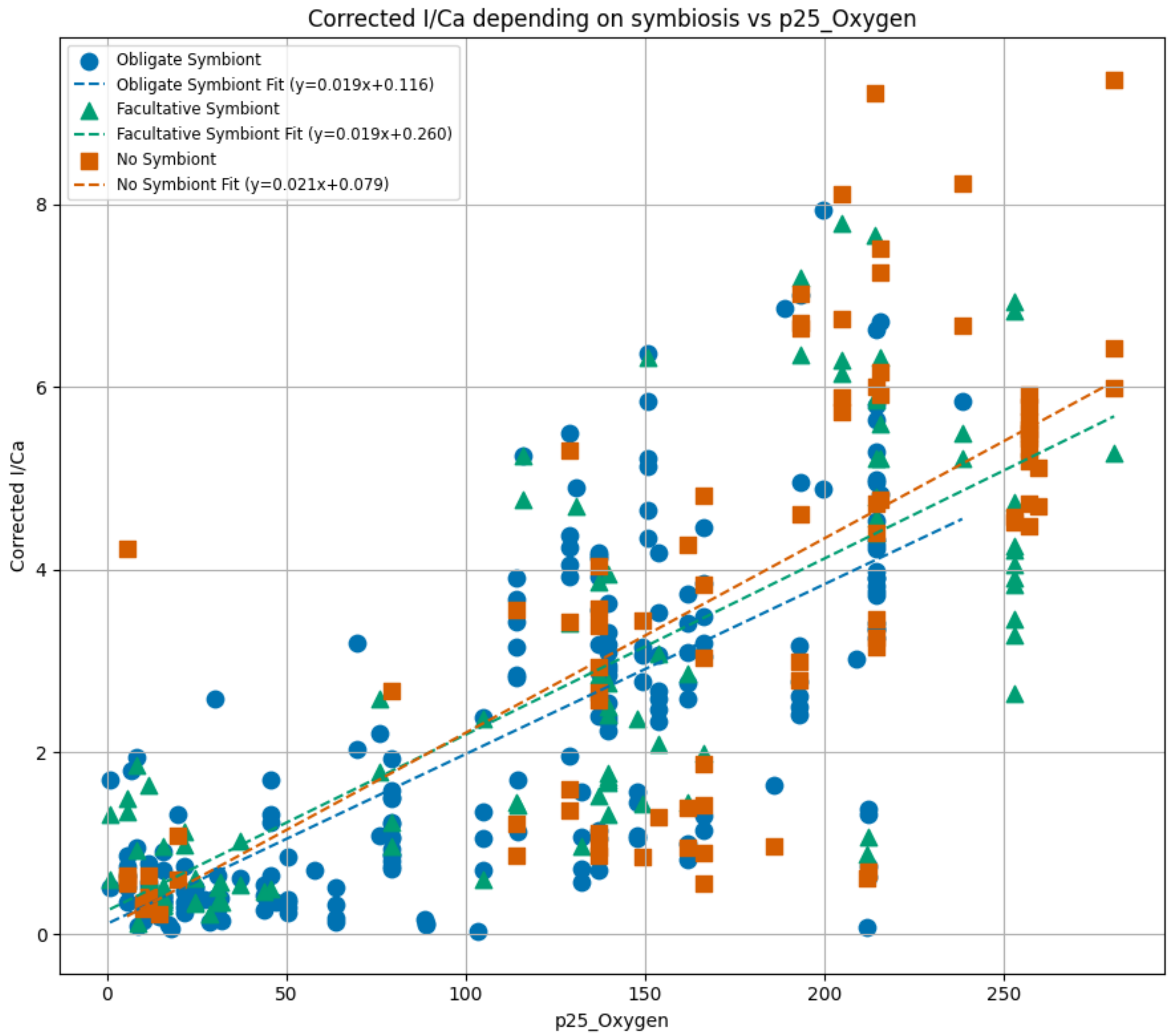

Figure S3: Foraminiferal I/Ca (µmol/mol) more recent than 2ka BP as a function of p25 oxygen (µmol/kg). Data were separated within 3 symbiosis groups from obligate symbiont (blue round), facultative symbiont (cyan triangles) and no symbiont (orange squares). Linear regressions are least absolute deviations and were calculated for each group. Regarding symbiont bearing/barren species, *Globorotalia menardii* was considered as facultative symbiont bearing species as previously (Hess et al., 2025). However, this facultative symbiont behaviour has been challenged (Takagi et al., 2019).

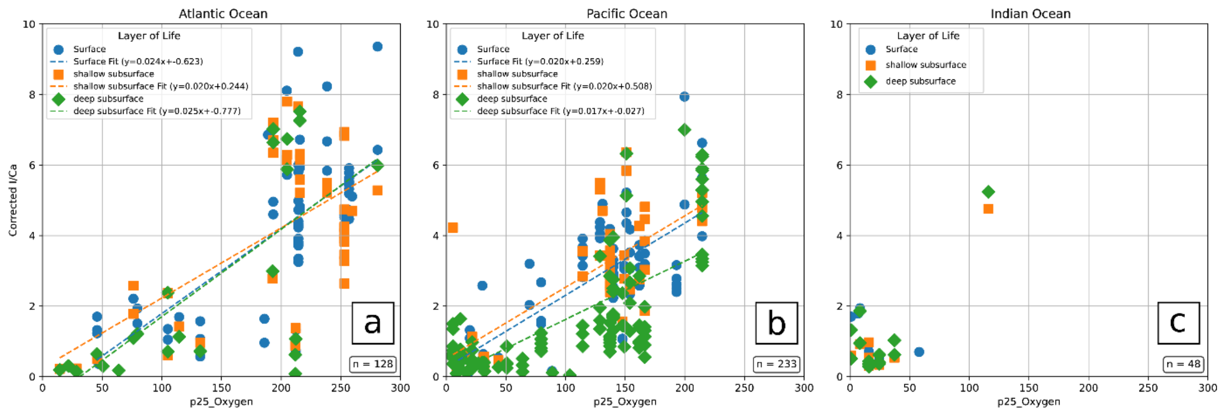

Figure S4: Foraminiferal I/Ca (µmol/mol) as a function of p25 oxygen (µmol/kg) for Atlantic (a), Pacific (b), and Indian (c) oceans. Data were separated within 3 calcification depth groups from Surface (blue round), shallow subsurface (orange square) and deep subsurface (green diamond) dwellers. Linear regressions are least absolute deviations and were calculated for each group. No regression is plotted on panel c due to the low number of data for p25 > 60 µmol/kg.

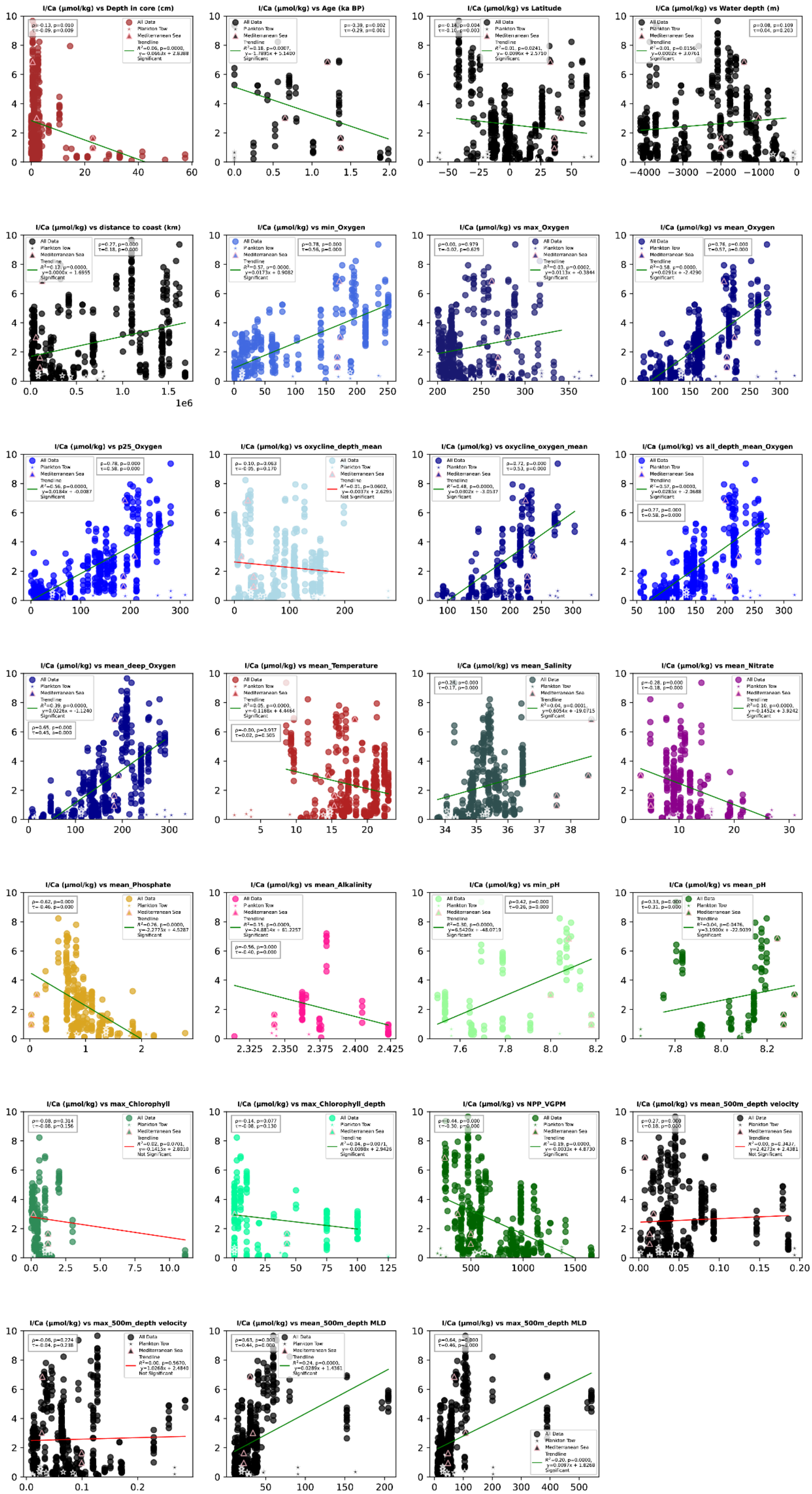
I/Ca (µmol/kg) vs Depth in core (cm)
I/Ca (µmol/kg) vs Age (ka BP)
I/Ca (µmol/kg) vs Latitude
I/Ca (µmol/kg) vs Water depth (m)
I/Ca (µmol/kg) vs distance to coast (km)
I/Ca (µmol/kg) vs min_Oxygen
I/Ca (µmol/kg) vs max_Oxygen
I/Ca (µmol/kg) vs mean_Oxygen
I/Ca (µmol/kg) vs p25_Oxygen
I/Ca (µmol/kg) vs oxycline_depth_mean
I/Ca (µmol/kg) vs oxycline_oxygen_mean
I/Ca (µmol/kg) vs all_depth_mean_Oxygen
I/Ca (µmol/kg) vs mean_deep_Oxygen
I/Ca (µmol/kg) vs mean_Temperature
I/Ca (µmol/kg) vs mean_Salinity
I/Ca (µmol/kg) vs mean_Nitrate
I/Ca (µmol/kg) vs mean_Phosphate
I/Ca (µmol/kg) vs mean_Alkalinity
I/Ca (µmol/kg) vs min_pH
I/Ca (µmol/kg) vs mean_pH
I/Ca (µmol/kg) vs max_Chlorophyll
I/Ca (µmol/kg) vs max_Chlorophyll_depth
I/Ca (µmol/kg) vs NPP_VGPM
I/Ca (µmol/kg) vs mean_500m_depth velocity
I/Ca (µmol/kg) vs max_500m_depth velocity
I/Ca (µmol/kg) vs mean_500m_depth MLD
I/Ca (µmol/kg) vs max_500m_depth MLD

Figure S5: Foraminiferal I/Ca (µmol/mol) as a function of different environmental parameters. Data and variables explored are presented and discussed in the main manuscript. Here we assumed linear correlation with green regression when the correlation is significant, and red when it is not.

We did not perform a Principal Component Analysis (PCA), as our objective was to evaluate the individual influence of each environmental variable on I/Ca rather than to reduce dimensions. Moreover, the presence of missing values could have biased the PCA with limited amount of data.

Secondary influence of multiple parameters, potentially related to iodine speciation

In order to identify secondary parameters that may influence the proxy. We use the Least Absolute Deviation regression from figure 5 to model foraminiferal I/Ca based on oxygen distribution and especially p25 [O_2] value at each site. The calculated residuals are then plotted against multiple ocean variables for each site. Table S1 summarises the correlation coefficients and significance of the parameters tested. Figure S6 presents residuals against the parameters tested for samples more recent than 2 ka BP only. This limit was set to obtain trend for recent variable values. We chose to only test the parameters that were shown as significant in table 2 and figure S5. We also have added water depth and age of the samples to discuss different theories about the incorporation of iodine, the gain during particle settling, and the diagenetic effect. We also add Mg/Ca from samples published in Hess et al. 2025.

Table S1: Correlation coefficients and significance for foraminiferal I/Ca residuals. Variables significant before residuals are highlighted with * in the first column. Other columns highlighted with * are the variables significant using I/Ca residuals.

Variable	n	Spearman's ρ	Spearman p-value	Kendall's τ	Kendall p-value
Age (ka BP)	61	-0.60	<0.01	-0.42	<0.01
mean_Alkalinity	71	0.42	<0.01	0.24	<0.01
mean_Nitrate	237	0.33	<0.01	0.23	<0.01
distance to coast (km)	406	0.31	<0.01	0.22	<0.01
min_pH	110	0.30	<0.01	0.23	<0.01
mean_500m_depth MLD	407	0.29	<0.01	0.20	<0.01
oxycline_oxygen_mean	224	0.29	<0.01	0.17	<0.01
max_Oxygen	407	0.23	<0.01	0.17	<0.01
mean_Temperature	390	-0.18	<0.01	-0.12	<0.01
Water depth (m)	407	-0.16	<0.01	-0.11	<0.01
NPP_VGPM	402	-0.16	<0.01	-0.10	<0.01
Mg/Ca	161	0.15	0.06	0.10	0.06
Latitude	407	-0.13	0.01	-0.08	0.02
max_Chlorophyll_depth	170	-0.10	0.20	-0.07	0.20
mean_Phosphate	267	-0.06	0.31	-0.03	0.40
mean_Salinity	390	0.06	0.28	0.04	0.29
min_Oxygen	407	0.05	0.31	0.00	0.96

all_depth_mean_Oxygen	404	0.04	0.38	0.01	0.73
max_500m_depth velocity	407	-0.04	0.38	-0.02	0.57
mean_Oxygen	407	0.03	0.57	0.01	0.88
p25_Oxygen	407	-0.01	0.79	-0.05	0.13
oxycline_depth_mean	377	-0.01	0.82	0.00	0.99

Oxygen variables are no longer highly correlated to foraminiferal I/Ca residuals, except oxygen at oxycline and maximum oxygen value at 0–500 m. This suggests that some oxygen variability component is still not perfectly constrained using linear calibration, or that seasonality or primary productivity can also influence the proxy's behaviour. It may be related to the relationship between oxygen and the non-linear inorganic iodine speciation, or to the incorporation mechanism. Those parameters are still poorly constrained and could be the source for secondary scattering. Linear calibration seems a good first order approximation, but further investigation on seasonality and iodine incorporation in calcite lattice will be highly needed to further constrain the proxy system.

Age of the sample is the highest correlation to residuals, with -0.63 and -0.45 for Spearman's and Kendall's coefficients respectively. But the figure S6A shows important scattering and only 74 points. Thus, the correlation is not as robust as parameters presenting more data points.

The effect of pH is important with correlation coefficients of 0.38 and 0.28 for Spearman's ρ and Kendall's τ respectively. This highlights a potential covariation with carbonate system, even if the scattering is important and the number of data limited with 110 points (Fig. S6O).

Other parameters such as temperature and Mg/Ca are also highlighted. Mg/Ca is a proxy for temperature and it has been used to obtain the calcification depth of foraminifera and remove its contribution to I/Ca proxy (Hess et al., 2025). The correlation coefficients are similar for the two parameters but opposite, when they should reflect similar parameter. No trend is visible on figure S6F and S6L.

A visible trend in residuals is the latitude. The pattern shows higher variability at high latitudes and less residuals closer to Equator (Fig. S6B). This pattern is very similar to iodide concentrations reported by Chance et al. (2020). The two behaviours are consistent as higher iodide concentration at low latitudes should be directly correlated with lower iodate concentrations, all this in relation with the presence of subsurface low oxygen waters. And this is also linked with less dispersion in I/Ca in oxygen depleted areas (p25 [O_2] <100 µmol/kg). The dispersion may also be partly related to the relation between oxygen and iodine speciation, and/or to area-specific iodine behaviour (Chance et al., 2020). The I/Ca residuals for water depth (Fig. S6C) does not present any trend. We note the same observation on distance to coast (Fig. S6D), even though the correlation with I/Ca residuals is high (Table S1). The two variables are not independent as shown in Figure S2. It is currently not possible to deconvolute the two parameters without further investigation on the relation between inorganic iodine speciation/concentration and foraminiferal I/Ca. But the complexity of the system, the scarcity of iodine speciation measures, and the lack of comparable couples of I/Ca with iodine speciation might be a source for the observed scattering.

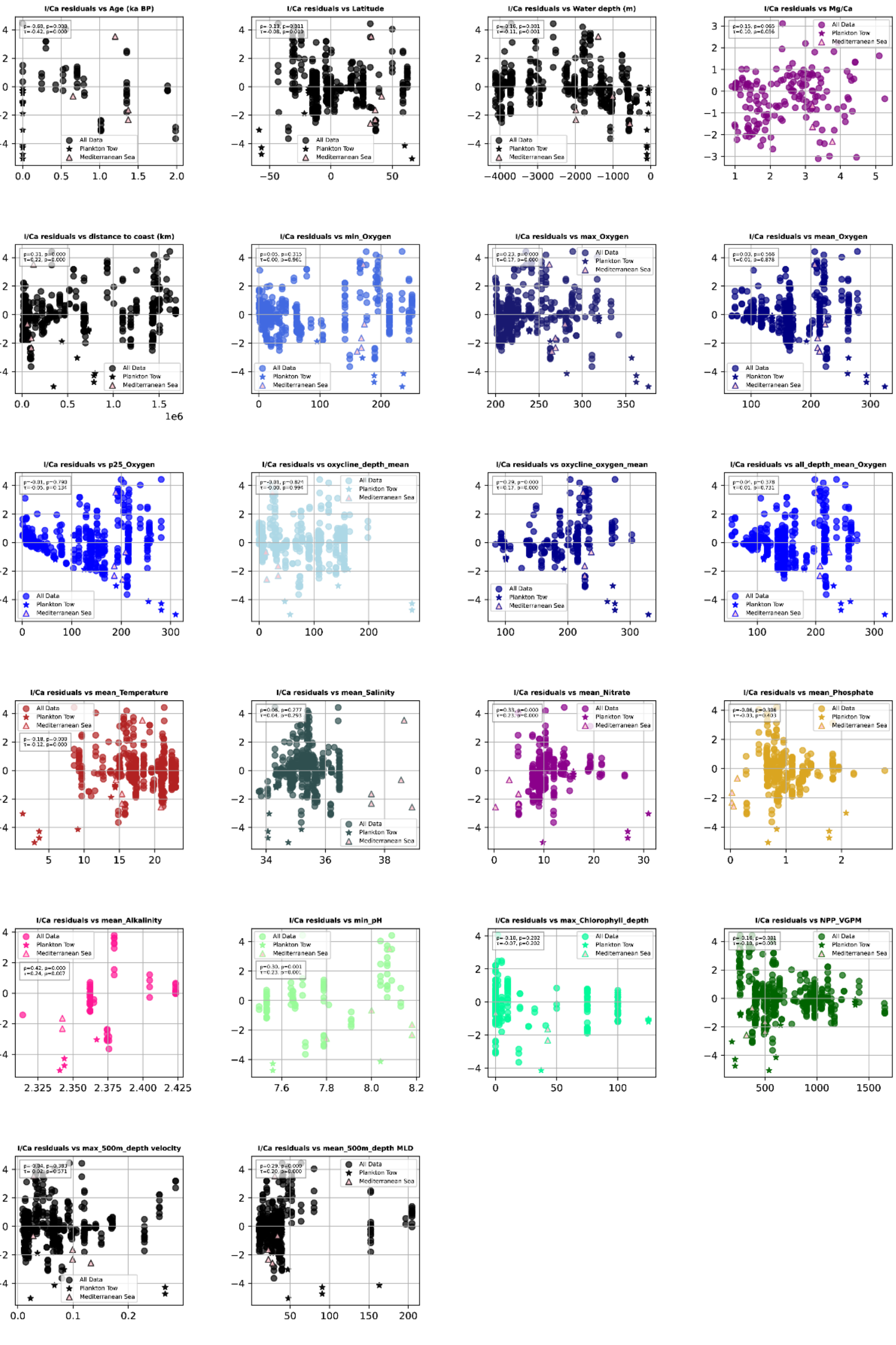

Figure S6: Foraminiferal I/Ca ratio residuals (µmol/mol) as a function of environmental parameters. Main oxygen contribution has been removed by using the proposed calibration. Mediterranean and plankton tow data have been separated from previously published dataset. Spearman's and Kendall's correlation coefficients and associated p-values are associated with each plot.

To summarise, foraminiferal I/Ca ratio does principally respond to oxygen concentration via inorganic iodine speciation and concentration. But it is still not clear which part of the water column is responsible for the signal.

The approximation of the first 500 m is useful to average the depth in which planktonic foraminifera are calcifying. But the proxy might be very sensitive to local inorganic iodine speciation, that is not fully constrained, and seems to be responsible for a lot of scattering. Further studies are highly needed to better understand the proxy.

The Mediterranean Sea is a semi-enclosed basin with its own thermohaline circulation driven by important evaporation within the whole basin (Millot and Taupier-Letage, 2005). This deficitary hydrological balance induces Atlantic water inflow through the Strait of Gibraltar. Winter wind driven deep water formation is located in the Gulf of Lion for the western basin, and in the Adriatic and Aegean Sea for the Eastern basin (Pinardi et al., 2015). This thermohaline circulation provides oxygen to depth (Rohling et al., 2015). MS is an oligotrophic basin with high productivity area limited to several coastal zones (Macias et al., 2018). Consequently, the MS is fairly well oxygenated, with mean oxygen concentrations ranging from 180 to 240 µmol/kg within the water column, and the western basin being slightly more oxygenated than the eastern basin (Mavropoulou et al., 2020).

Mediterranean Sea foraminiferal I/Ca core top range from 0.6 to 7 µmol/mol. However, p25 oxygen values at subsurface are close to 200 µmol/kg at studied sites (Fig. 3). The calibration indicates expected I/Ca values of 3.5 µmol/mol. This important dispersion cannot be attributed to specie specific processes as different depth dwellers show close I/Ca ratio for a same site (Fig. S2). This could suggest an influence of seasonal iodine speciation variability at studied sites as foraminifera living at different times of the year shows ∼77% maximum variability. However, seasonal iodate concentration variability is ∼22% in the north-western MS (Tian and Nicolas, 1995).

Our data also present an absence of relation between iodine in foraminifera and sampling depth. Shallower core site, MD99-2341 at 577 mbsl in Gulf of Cadiz, has the lowest foraminiferal I/Ca around 0.65 µmol/mol with p25 [O_2] being 212 µmol/kg. Deepest core, ODP Site 977 at 1984 mbsl, presents very low I/Ca with values below 1µmol/mol in oxygenated waters (p25 [O_2] = 186 µmol/kg). From our results, low I/Ca values are found closer to the strait of Gibraltar, indicating a potential contribution of Atlantic water to iodate depletion. Scarce iodine speciation and foraminiferal I/Ca data were not sufficient to identify specific behaviour in MS or Atlantic.

Moreover, no evidence of important temperature, salinity or other parameter influence could be noted from figure S6. Mediterranean basin-specific characteristics are therefore not expected to hinder the application of the proxy. Our results indicate that, in the MS as well as in the global ocean, oxygen remains the dominant factor controlling via its influence on iodine speciation. The magnitude of the observed scatter ∼6 µmol/mol) is comparable to that found in the rest of the global dataset (∼7 µmol/mol). However, semi-enclosed basins might limit the number of available records of open-ocean type cores not influenced by coastal effects and be more sensitive do iodine concentration changes. Western basin proxy-based oxygenation state reconstruction appears challenging as no high I/Ca was found in core top samples. But those observation might be linked to area specific processes. This could explain the observed anomaly in the gulf of Cadiz and Alboran Sea. As Hess et al. 2025 recommended, foraminiferal I/Ca ratio from near continent or restricted basin sites should be handled carefully, as some specifics mechanisms of iodine speciation or incorporation might occur. It is especially true for the MS.

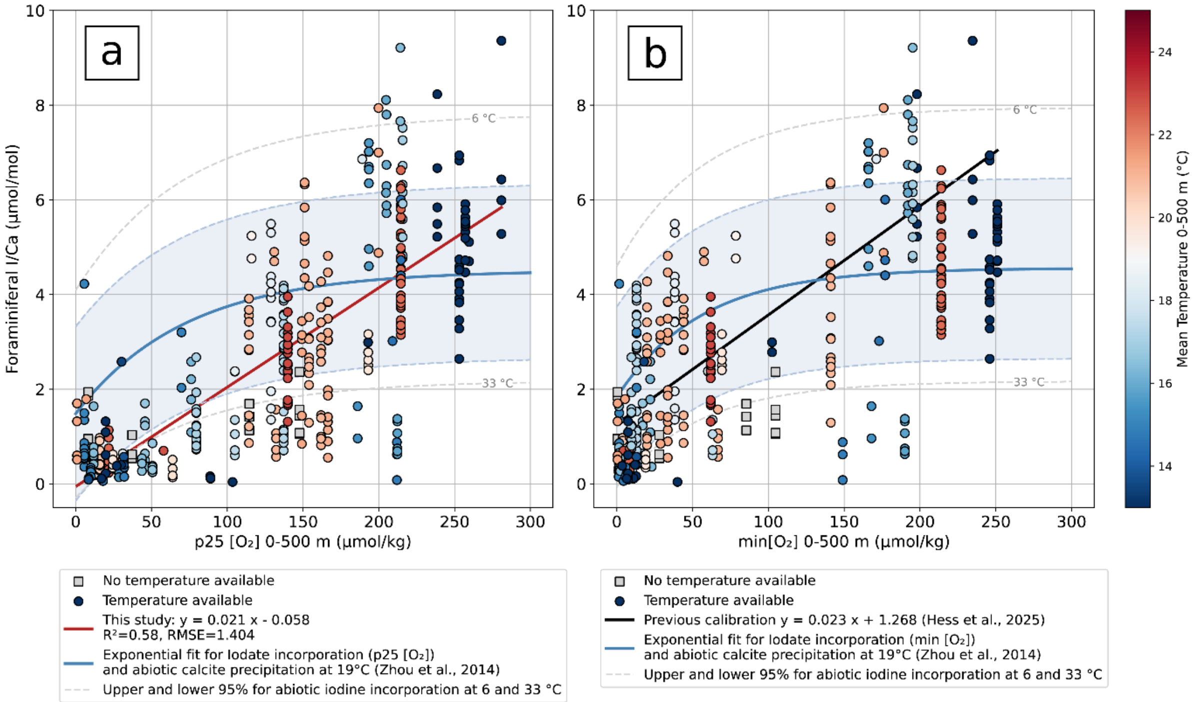

Figure S7: Foraminiferal I/Ca <2 ka BP as a function of p25 [O2] (a) and min[O2] (b) in 0–500 m. The red line is the linear model proposed in this study. Blue curve represents the abiotic incorporation of iodine following iodate proportion in total inorganic iodine determined in Figure 3 and assuming a mean concentration of total inorganic iodine of 471 nM (Fig. 3c). The abiotic incorporation was determined following (Zhou et al., 2014). Blue area corresponds to 95% prediction interval also determined in Figure 4 for a temperature of 19 °C. 57% of the data fall in this prediction interval. Temperature from 6 to 33 °C are considered for the maximum and minimum 95% prediction interval with total iodine concentration of 471 nM (grey dashed lines).

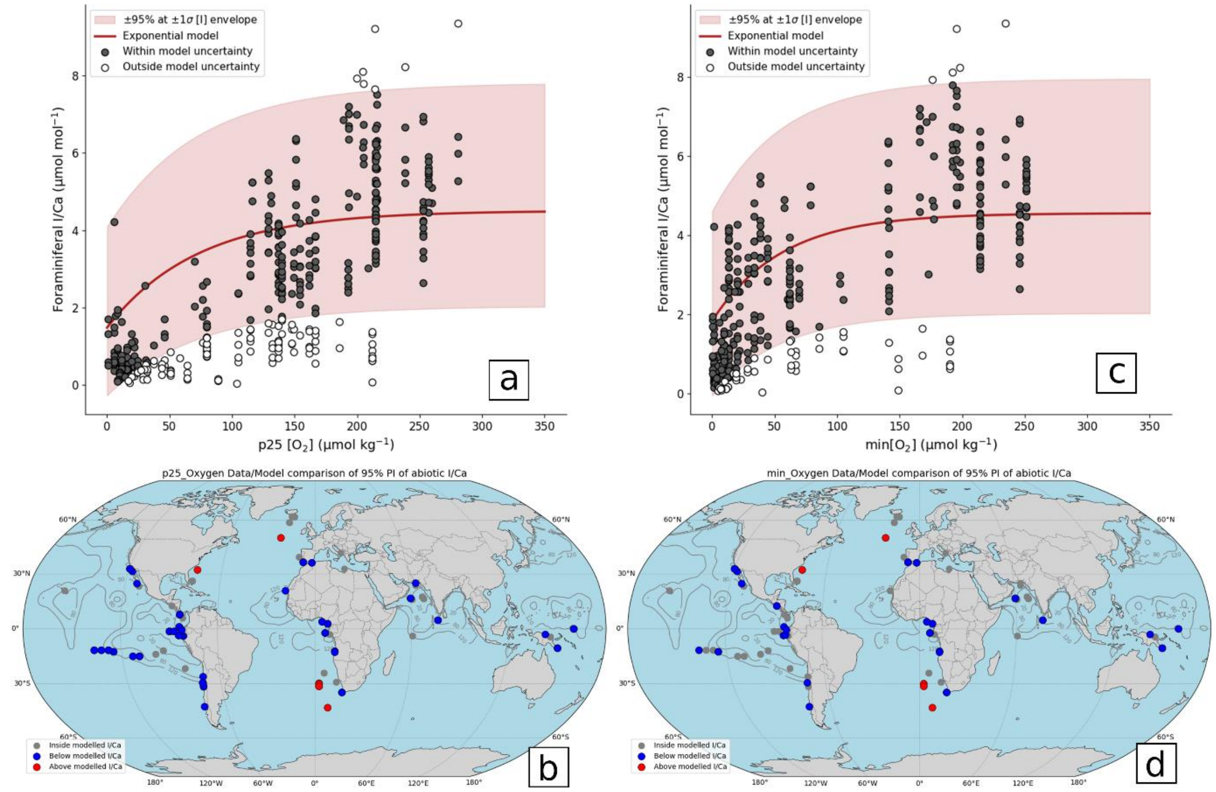

Figure S8: Foraminiferal I/Ca ratio (µmol/mol) as a function of p25 [O_2] (a) and minimum [O_2] (c). Red curve is the exponential model based on iodate proportion (Fig. 3a) and inorganic iodine incorporation at 19°C (Zhou et al., 2014). The red shaded area corresponds to the 95% prediction interval of the iodate proportion with total inorganic iodine concentration at ±1σ (Fig. 3c). Points that fall into the model uncertainty are in grey. Others are plotted in white. Maps represent data above (red) and below (blue) 95% prediction interval of modelled abiotic I/Ca for p25 (b) and minimum (d) [O_2]. Grey lines represent the presence of low oxygen concentration (20, 80 and 120 µmol/kg) in 0–500 m.

References

Chance, R., Tinel, L., Sarkar, A., Sinha, A. K., Mahajan, A. S., Chacko, R., Sabu, P., Roy, R., Jickells, T. D., Stevens, D. P., Wadley, M., and Carpenter, L. J.: Surface Inorganic Iodine Speciation in the Indian and Southern Oceans From 12°N to 70°S, Front. Mar. Sci., 7, 621, https://doi.org/10.3389/fmars.2020.00621, 2020.

Hess, A. V., Rosenthal, Y., Zhou, X., and Bu, K.: The I/Ca paleo-oxygenation proxy in planktonic foraminifera: A multispecies core-top calibration, Geochim. Cosmochim. Acta, S0016703725000298, https://doi.org/10.1016/j.gca.2025.01.018, 2025.

Macias, D., Garcia-Gorriz, E., and Stips, A.: Major fertilization sources and mechanisms for Mediterranean Sea coastal ecosystems: Fertilization of Mediterranean coasts, Limnol. Oceanogr., 63, 897–914, https://doi.org/10.1002/lno.10677, 2018.

Mavropoulou, A.-M., Vervatis, V., and Sofianos, S.: Dissolved oxygen variability in the Mediterranean Sea, J. Mar. Syst., 208, 103348, https://doi.org/10.1016/j.jmarsys.2020.103348, 2020.

Millot, C. and Taupier-Letage, I.: Circulation in the Mediterranean Sea, in: The Mediterranean Sea, vol. 5K, edited by: Saliot, A., Springer Berlin Heidelberg, Berlin, Heidelberg, 29–66, https://doi.org/10.1007/b107143, 2005.

Pinardi, N., Zavatarelli, M., Adani, M., Coppini, G., Fratianni, C., Oddo, P., Simoncelli, S., Tonani, M., Lyubartsev, V., Dobricic, S., and Bonaduce, A.: Mediterranean Sea large-scale low-frequency ocean variability and water mass formation rates from 1987 to 2007: A retrospective analysis, Prog. Oceanogr., 132, 318–332, https://doi.org/10.1016/j.pocean.2013.11.003, 2015.

Rohling, E. J., Marino, G., and Grant, K. M.: Mediterranean climate and oceanography, and the periodic development of anoxic events (sapropels), 36, 2015.

Takagi, H., Kimoto, K., Fujiki, T., Saito, H., Schmidt, C., Kucera, M., and Moriya, K.: Characterizing photosymbiosis in modern planktonic foraminifera, Biogeosciences, 16, 3377–3396, https://doi.org/10.5194/bg-16-3377-2019, 2019.

Tian, R. C. and Nicolas, E.: Iodine speciation in the northwestern Mediterranean Sea, method and vertical profile, Mar. Chem., 48, 151–156, https://doi.org/10.1016/0304-4203(94)00048-I, 1995.

Zhou, X., Thomas, E., Rickaby, R. E. M., Winguth, A. M. E., and Lu, Z.: I/Ca evidence for upper ocean deoxygenation during the PETM, Paleoceanography, 29, 964–975, https://doi.org/10.1002/2014PA002702, 2014.